ARTICLES

Chemical Functionalization of Magnetic Carbon-Encapsulated Nanoparticles Based on Acid Oxidation

Yanwen Ma, Zheng Hu,* Leshu Yu, Yemin Hu, Bing Yue, Xizhang Wang, and Yi Chen

Key Laboratory of Mesoscopic Chemistry of MOE and Jiangsu Provincial Lab for NanoTechnology, School of Chemistry and Chemical Engineering, Nanjing University, Nanjing 210093, China

Yinong Lu

College of Materials Science and Engineering, Nanjing University of Technology, Nanjing 210093, China

Yang Liu[†] and Junhui Hu[†,‡]

Shenzhen Junye Nano Material Co., Ltd., Shenzhen, 518118, China, and State Key Lab of Plastic Forming Simulation, and Die and Mould Technology, Department of Materials Science and Engineering, Huazhong University of Science and Technology, Wuhan 430074, China

Received: May 15, 2006; In Final Form: August 10, 2006

Carbon-encapsulated nickel nanoparticles were used as the representative magnetic carbon-encapsulated nanoparticles for chemical functionalization. After oxidation with the mixed acid of H_2SO_4/HNO_3 under a moderate ultrasonic bath, carboxylic acid groups (−COOH) were effectively generated on the fullerene-like carbon shells, which in turn were utilized to covalently link octadecylamine through an amide reaction. The whole chemical process is well characterized by many methods such as Fourier transform infrared spectroscopy, X-ray photoelectron spectroscopy, thermogravimetry-differential scanning calorimetry, transmission electron microscopy, and so on, and the self-consistent experimental results were obtained. The results suggested that the magnetic nanoparticles could be well protected, while their magnetic properties could be utilized to guide the transfer of the grafted functional species on the particle surface. This provides many possibilities for potential applications in chemical and biochemical fields.

1. Introduction

Carbon-encapsulated nanoparticles (CENPs),[1,2] classified as "giant fullerenes" for their outer fullerene-like graphite shells,[3] have attracted much attention since such nanostructures could protect the encapsulated nanoparticles from environmental degradation. In the past decade, many substances such as rare earth elements,[1,2] metals,[4−10] and their carbides[9,11] have been successfully encapsulated. In these CENPs, the magnetic CENPs which usually contain the ferromagnetic Fe,[6,9] Ni,[5−7,10] Co,[5,7,8] or their alloy[12] nanoparticles inside constitute a group of especially interesting nanomaterials due to their higher chemical stability toward air-oxidation and acid-dissolution in comparison with the naked ferromagnetic nanoparticles, and the magnetic properties of the inside ferromagnetic nanoparticles could be well protected by such nanostructures.[8,10] These magnetic CENPs are now regarded as promising candidates in many applications ranging from data storage and xerography for information techniques[13] to drug delivery and magnetic resonance for biomedicines.[14] It is known that the generation of functional groups onto the magnetic nanoparticles' surfaces is of considerable significance for connecting targeting ligands, drugs, peptides, and antibodies in biochemistry, medicine, and biotechnology.[15−18] For examples, vancomycin-functionalized FePt nanoparticles are amazing pathogen detectors,[17] and hydroxyl group-modified magnetite nanoparticles (Fe_3O_4−OH) could effectively attach human immunoglobulin.[18] It is understood that the functionalized magnetic nanoparticles via directly modifying the corresponding naked ones are greatly influenced by environmental factors such as temperature, pH, and the functional groups' response. These could result in instability, large aggregation, and rapid biodegradation when they are exposed to the biological system, hence difficult for practical applications.[19] It seems that such drawbacks could be prevented by replacement of the naked magnetic nanoparticles by the carbon-encapsulated ones, since the intrinsic properties of the inner magnetic cores in this case are well-protected by the outer carbon shells, which in turn provides many possibilities for further modification. However, the studies on CENPs have concentrated mostly on the synthesis and characterization to date, and little is known about their further chemical modification,[20] probably due to the difficulty of obtaining a large enough quantity of such CENPs. By laser-induction complex heating evaporation synthesis,[21] we could produce carbon-encapsulated

* Corresponding author. Tel: 0086-25-83686015. Fax: 0086-25-83686251. E-mail address: zhenghu@nju.edu.cn.
[†] Shenzhen Junye Nano Material Co., Ltd.
[‡] Huazhong University of Science and Technology.

10.1021/jp062957f CCC: $33.50
Published on Web 09/02/2006

nickel nanoparticles [Ni(C) nanocapsules] at approximately the kilogram level, which provide us the possibility of studying the chemical functionalization of such magnetic CENPs.

It is noticed that chemical functionalization of carbon nanotubes (CNTs) has been well studied, and some effective methods have been developed.[22] Due to the structural similarity between the graphite shells of CENPs and CNTs, these methods should be applicable to the chemical functionalization of CENPs through suitable modification. Acid oxidation could generate oxygen-containing groups such as hydroxyl (−OH) and carboxylic acid groups (−COOH) at CNTs' defective sides.[23−26] In this paper, chemical functionalization of Ni(C) nanocapsules was realized by nitric and sulfuric acid oxidation, and the sequentially generated chemical activity was well demonstrated by octadecylamine grafting.

2. Experimental Section

Synthesis of Ni(C) Nanocapsules. The pristine Ni(C) nanocapsules were produced by laser-induction complex heating evaporation synthesis as described in our previous paper.[27] The as-prepared samples were fully washed with concentrated hydrochloric acid (HCl, 12 mol L^{-1}) for dissolving the unencapsulated Ni nanoparticles, then washed with distilled water several times, and finally dried at 70 °C for further study.

Acid Oxidation of Ni(C) Nanocapsules. In a typical run, a 1-g amount of Ni(C) nanocapsules was suspended in a 90-mL mixture of concentrated H_2SO_4 (18 mol L^{-1})/HNO_3 (16 mol L^{-1}) with the ratio of 2:1 and sonicated in a water bath (40 kHz, 70 W) for 2 h. The above solution was then diluted by 1 L of distilled water and deposited for 12 h. The sample in the solution was separated into two fractions, that is, a portion floating on the solution surface and that depositing to the bottom. The floater and the precipitate were collected by centrifuging with rotating speeds of 9000 and 3000 rpm, respectively. Both samples were washed with distilled water through several periods of the washing−centrifuging process until the pH value of 7 was reached for the centrifugal liquid, and they were finally dried under vacuum for 12 h at room temperature. The yields of the floater and the precipitate are about 0.03 and 0.18 g, respectively. The precipitates obtained were oxidized Ni(C) nanocapsules, which were used for the further chemical functionalization.

Octadecylamine-Grafted Ni(C) Nanocapsules. An amount of 0.18 g of oxidized Ni(C) nanocapsules [Ni(C)−COOH] was suspended in 20 mL of distilled $SOCl_2$ together with 1 mL of dimethylformamide at 70 °C for 24 h. This could result in the formation of acid chloride-modified Ni(C) nanocapsules [Ni(C)−COCl] which was then separated by centrifuging and washed with anhydrous tetrahydrofuran. After drying under vacuum at room temperature for 4 h, the sample (about 0.16 g) was mixed with 2 g of octadecylamine (ODA, Aldrich) and heated at about 95 °C for 96 h. After cooling to room temperature, the excess ODA was removed by repeated washing with ethanol and centrifuging (3000 rpm). The remaining sample was dried under vacuum overnight, and about 0.20 g of sample was obtained [noted as Ni(C)−ODA].

Sample Characterization. X-ray diffraction (XRD) experiments were carried out on a Philips X'pert Pro X-ray diffractometer with Cu Kα radiation of 1.5418 Å. The morphology and structure of the product were analyzed by transmission electron microscopy (TEM, JEOL-JEM-1005 at 100 kV) and high-resolution transmission electron microscopy (HRTEM, JEM2010 at 200 kV) equipped with an energy-dispersive X-ray spectrometer (EDX, ThermoNORAN). The magnetic hysteresis loop was measured by a vibrating sample magnetometer in the range of −8000 to 8000 Oe at room temperature. The functional groups were detected by Fourier transform infrared spectroscopy (FTIR, BRUKER VECTOR22) with a KBr pressed pellet and X-ray photoelectron spectroscopy (XPS, ESCALab MK-II).

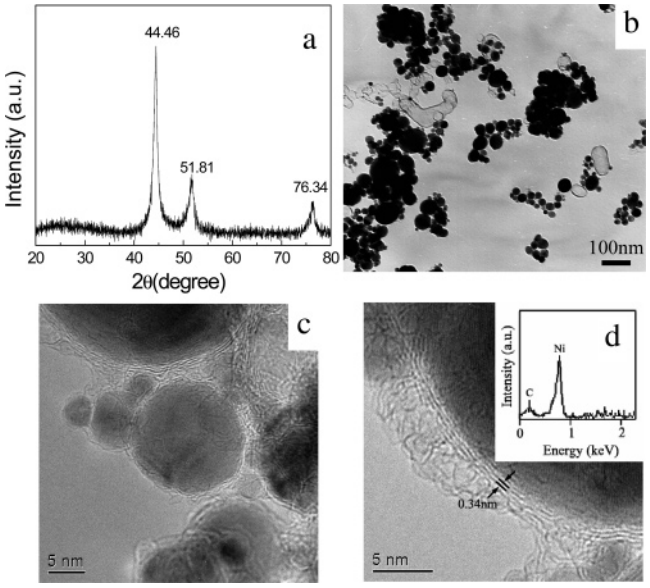

Figure 1. XRD curve (a), TEM (b), and HRTEM (c, d) images of Ni(C) nanocapsules. The insert in (d) is the corresponding EDX spectrum.

Thermogravimetry (TG, NETZSCH STA-499C)-mass spectrum (MS, PFEIFFER QUADSTAR-422) and thermogravimetry-differential scanning calorimetry (TG-DSC) profiles were recorded with a 10 °C/min heating rate in Ar from about 30 °C to the preselected temperature.

3. Results and Discussion

The XRD curve for a sample of Ni(C) nanocapsules is shown in Figure 1a. Three peaks around 44.46°, 51.81°, and 76.34° correspond to the reflection lines of the face-centered cubic phase of Ni (JCPDS, No. 04-0850); however, no graphite signals are observed. The typical TEM image in Figure 1b shows that the Ni(C) nanocapsule sample is composed mainly of solid particles with the size range 5−100 nm. A few hollow nanostructures in the sample should be the hollow carbon nanocages due to the core-dissolving of the uncompacted Ni(C) nanocapsules after the HCl erosion. Figure 1c,d shows the HRTEM images of the Ni(C) nanocapsules. It is seen that the nanocapsules have core/shell structures, and the outer shell is composed of several graphite layers of a few nanometers in thickness, with a spacing between two neighboring lattice fringes of ∼0.34 nm corresponding to the d_{002} of graphite. These thin shells have low graphitic crystalline degree and even amorphous carbon structure, resulting in an undetectable graphite signal in the XRD curve. The corresponding EDX analysis inserted in Figure 1d further indicates that the nanoparticles consist of inner nickel cores and outer carbon shells.

The hysteresis loop is shown in Figure 2. The saturation magnetization (M_z), remanent magnetization (M_r) and coercivity (H_c) values are about 30 emu/g, 6 emg/g, and 140 Oe, respectively, reflecting the soft ferromagnetic characteristics at room temperature due to the encapsulated Ni particles. In comparison with the M_z value of the bulk Ni (∼50 emu/g), the relative lower saturation magnetization for the Ni(C) nanocapsules (∼30 emu/g) resulted from the coexistence of the

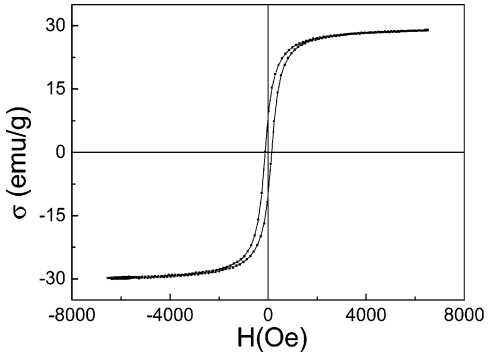

Figure 2. Magnetic hysteresis loop of the Ni(C) nanocapsules.

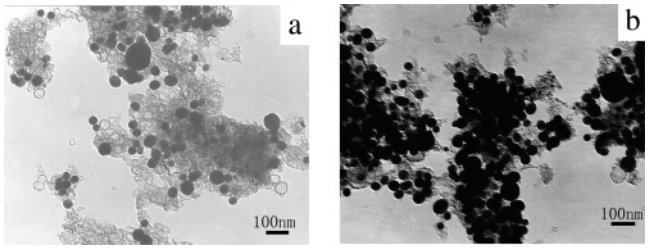

Figure 3. Typical TEM images of the Ni(C) nanocapsules after acid oxidation. Specimens from solution (a), and specimens from precipitate (b).

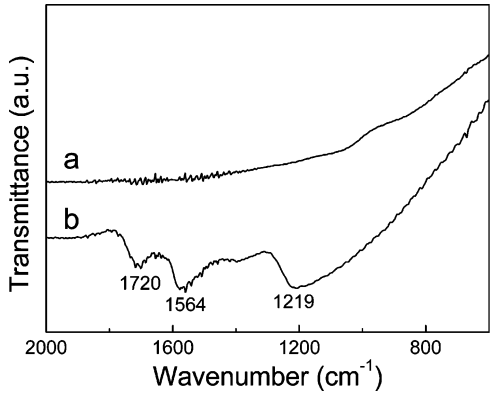

Figure 4. FTIR spectra of Ni(C) nanocapsules before (a) and after acid oxidation (b).

nonmagnetic carbon shell and the large percentage of surface spin with disordered magnetization orientation for nanosized particles.[10]

After the acid oxidation, only about 18 wt % of oxidized Ni(C) nanocapsules remained, and the rest were opened and the inside Ni cores dissolved as learned from our earlier study.[27] The herein generated hollow carbon nanocages (as shown in Figure 3a) floated on the solution and were separated from the solid sample through precipitation. In this way, oxidized Ni(C) nanocapsules were thus obtained (Figure 3b). FTIR spectra of the Ni(C) nanocapsules before and after oxidation treatment are shown in Figure 4. It is found that three new peaks around 1720, 1564, and 1219 cm^{-1} appeared after the oxidation treatment; these peaks can be assigned to C═O in COOH, C═C in the graphite skeleton, and the C−C stretching vibration, respectively,[28] indicating that the acid oxidation can expose the graphite layers by removing the amorphous carbon, following the generation of −COOH groups.

XPS analysis could provide additional information about the oxygen-containing surface groups. Figure 5a shows the C1s XPS peaks of the Ni(C) nanocapsules before and after oxidation treatment. The curve for the untreated Ni(C) nanocapsules shows

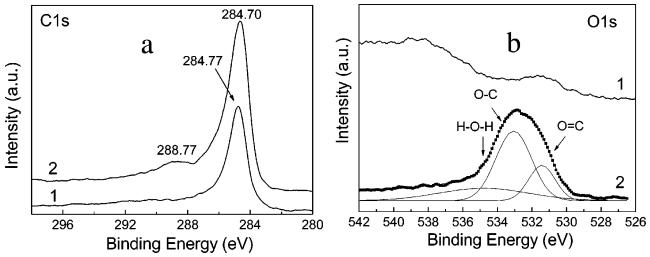

Figure 5. XPS spectra of Ni(C) nanocapsules before (1) and after acid oxidation (2). (a) C1s peaks, (b) O1s peaks.

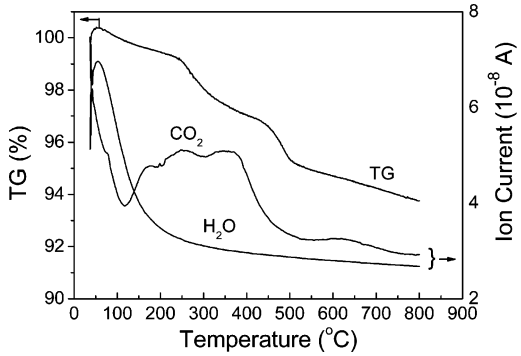

Figure 6. TG-MS profile of the oxidized Ni(C) nanocapsules.

a dominant peak structure for the C1s core level at a binding energy of 284.77 eV, corresponding to the carbon shells of Ni-(C) nanocapsules in reference to the XPS studies on CNTs.[26,29,30] For the oxidized Ni(C) nanocapsules, the C1s line has an obvious broader full width at half-maximum than that of the untreated sample via extending the peak at the high-binding-energy side, attributed to the effect of functional groups.[30a] A prominent raised bump around 288.77 eV, similar to that for oxidized CNTs, is caused by the −COO− functional group.[30a] The corresponding O1s line in Figure 5b clearly demonstrates that the oxidized Ni(C) nanocapsules give a much enhanced O1s signal at 532.84 eV. Referring to the XPS studies on the acid-oxidized carbon nanotubes,[26,30b] the O1s signal here could be attributed to the contribution of O═C at 531.44 eV, O−C at 533.12 eV, and H−O−H at 534.78 eV, respectively, as indicated in Figure 5b. It is seen that the intensity for H−O−H is much lower than that for O═C and O−C. This suggests that the O1s signal of the oxidized Ni(C) nanocapsules arises mainly from the carboxyl groups rather than from the physisorbed water, which is further supported by our TG-MS analysis of the sample as shown in Figure 6. As seen from the TG curve, the weight loss occurred in almost the whole temperature region. From the corresponding MS curves for H_2O and CO_2 fragments, it could be learned that the weigh loss in the TG curve below 150 °C was caused mainly by the desorption of the physisorbed water[31] (intensive H_2O signal and weak CO_2 signal), and that in the range of 150−400 °C was caused mainly by the decomposition of the carboxyl groups[31] (intensive CO_2 signal and weak H_2O signal). From the TG curve, it could also be estimated that, in the range of 30−400 °C, about 80% weight loss came from the decomposition of the carboxyl groups. This weight loss indicates the effective generation of a large quantity of carboxyl groups on the surface of Ni(C) nanocapsules after oxidation treatment, in agreement with the XPS analysis results (Figure 5).

The successful functionalization of −COOH groups on the surface of the Ni(C) nanocapsules provides us with the further possibility of linking different targeting species. We tried to graft ODA onto the oxidized Ni(C) nanocapsules for end

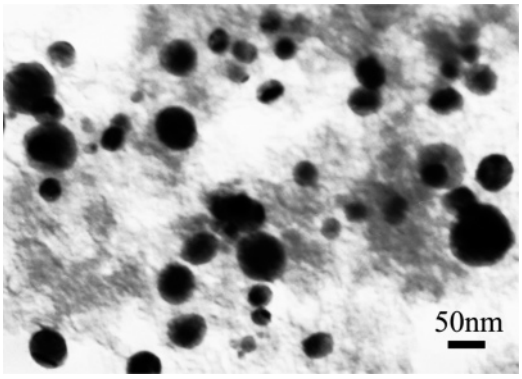

Figure 7. Typical TEM image of Ni(C)-ODA.

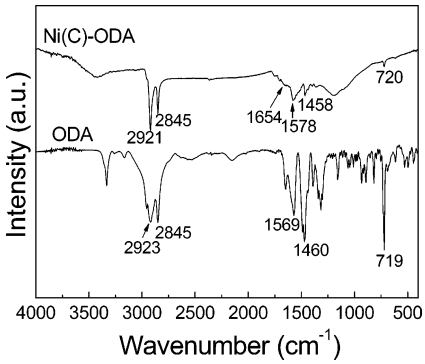

Figure 8. FTIR spectra of ODA and Ni(C)-ODA.

amidation through the following chemical process:

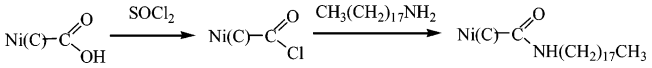

Figure 7 is the typical TEM image of the Ni(C)-ODA. It is notable that the particles are wrapped by a layer of polymer-like materials with varying thickness. The impurities should be caused by the carbon segments not washed out. Figure 8 shows a comparison of the FTIR spectra for ODA and our Ni(C)-ODA samples. Their similarity indicates the effective grafting of ODA onto Ni(C) nanocapsules. The peaks at 2921 and 2845 cm^{-1} for Ni(C)-ODA come from the C−H stretching vibrations, and the peaks at 1458 and 720 cm^{-1} arise from the C−H bending and rocking vibrations of the alkyl chain, respectively. In particular, the characteristic peak for the amide carbonyl group appears around 1654 cm^{-1}, indicating the covalent bonding of ODA with the oxidized Ni(C) nanocapsules. The peak at 1578 cm^{-1} is probably due to the N−H bend of the amide in the final product, corresponding to 1569 cm^{-1} in ODA.[25]

The ODA-grafting onto Ni(C) nanocapsules was further supported by TG-DSC characterization of the Ni(C)-ODA sample as shown in Figure 9. For comparison, the TG curves for Ni(C) nanocapsules are also presented there. It is seen that the TG curve of the Ni(C) nanocapsules displays a slight weight gain when approaching 486 °C (curve a), which should be caused by the oxidation of the trace uncompactly encapsulated Ni nanoparticles by the O_2 impurity in the Ar carrier gas. The following weigh loss (ca. 10%) corresponds to the slow oxidation of the carbon shells to gaseous carbon oxide. For the TG curve of the Ni(C)-ODA (curve b), the onset of the weight loss at 240 °C is much lower than that for Ni(C) nanocapsules (curve a, about 486 °C), and a significant weight loss (about 30%) occurred in the range of 240−490 °C, suggesting the decomposition of the surface organics in this temperature range.[32,33] The following changing trend is quite similar to that

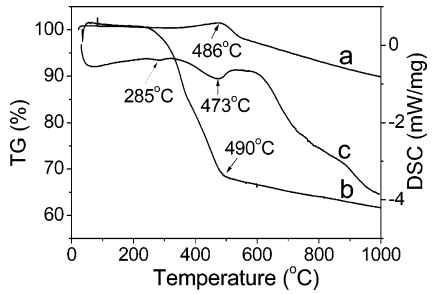

Figure 9. TG curves of Ni(C) nanocapsules (a) and Ni(C)-ODA (b), and the corresponding DSC curve for Ni(C)-ODA (c).

of Ni(C) nanocapsules (curve a), which should also arise from the oxidation of carbon shells. In the DSC curve for Ni(C)-ODA, there exist two endothermal peaks at 285 and 473 °C (curve c), which could be attributed to the decomposition of the physisorbed and covalently bonded ODA, respectively.[32,33] All these results are in agreement with those from Figures 7 and 8. These experimental results demonstrate that the surface of the Ni(C) nanocapsules could be functionalized with −COOH groups by acid oxidation, which could in turn covalently link ODA molecules. In the whole functionalization process, the functional groups are grafted on the surface of the carbon shells, which should not affect the inside Ni nanoparticles. The intuitionistic magnetic characteristics of the Ni(C) nanocapsules before and after fuctionalization are demonstrated by the magnetic attraction observation (see Supporting Information), suggesting that the ferromagnetism of Ni nanoparticles are well protected during the functionalization.

After the acid oxidation and the following ODA-grafting, the dispersion and the hydrophobicity of the Ni(C) nanocapsules were roughly assessed by dispersing the samples into a hexane/water solution. It is found that the ODA-grafting could obviously improve the dispersion of Ni(C) nanocapsules in hexane, and the raw Ni(C) nanocapsules can be modified from hydrophobicity to hydrophilicity by acid oxidation, and then back to the hydrophobicity by the ODA-grafting (see Supporting Information).

4. Conclusion

Carbon-encapsulated nickel nanoparticles were used as the representative magnetic CENPs for chemical functionalization. After oxidation with a mixture of H_2SO_4 and HNO_3 under a moderate ultrasonic bath, carboxylic acid groups (−COOH) were effectively generated on the fullerene-like carbon shells, which in turn were utilized to covalently link octadecylamine through an amide reaction. The self-consistent experimental results were obtained by different characterizations. The results suggested that the magnetic nanoparticles could be well protected while their magnetic properties were utilized to guide the transfer of the grafted functional species on the particle surface. This provides many possibilities for potential applications in chemical and biochemical fields.

Acknowledgment. This work was financially supported by NSFC (Nos. 20525312, 20471028), "863" Project (No. 2003AA302150), MOE (NCET-04-0449), The HwaYing Education and Culture Foundation, as well as Jiangsu Planned Projects for Postdoctoral Research Funds.

Supporting Information Available: The dispersion, hydrophobicity, and magnetic separation of the Ni(C) nanocapsules in a hexane/water solution before and after chemical function-

alization (PDF). This material is available free of charge via the Internet at http://pubs.acs.org.

References and Notes

(1) Ruoff, R. S.; Lorents, D. C.; Chan, B.; Malhotra, R.; Subramoney, S. *Science* **1993**, *259*, 346.

(2) Tomita, M.; Saito, Y.; Hayashi, T. *Jpn. J. Appl. Phys.* **1993**, *32*, L280.

(3) McHenry, M. E.; Majetich, S. A.; Artman, J. O.; DeGraef, M.; Staley, S. W. *Phys. Rev. B* **1994**, *49*, 11358.

(4) (a) Saito, Y.; Nishikubo, K.; Kawabata, K.; Matsumoto, T. *J. Appl. Phys*. **1996**, *80*, 3062. (b) Ugarte, D. *Chem. Phys. Lett*. **1993**, *209*, 99. (c) Uo, M.; Tamura, K.; Sato, Y.; Yokoyama, A.; Watari, F.; Totsuka, Y.; Tohji, K. *Small* **2005**, *1*, 816.

(5) Jiao, J.; Seraphin, S. *J. Appl. Phys.* **1998**, *83*, 2442.

(6) Si, P. Z.; Zhang, Z. D.; Geng, D. Y.; You, C. Y.; Zhao, X. G.; Zhang, W. S. *Carbon* **2003**, *41*, 247.

(7) Ling, J.; Liu, Y.; Hao, G.; Zhang, X. *Mater. Sci. Eng. B* **2003**, *100*, 186.

(8) Flahaut, E.; Agnoli, F.; Sloan, J.; O'Connor, C.; Green, M. L. H. *Chem. Mater*. **2002**, *14*, 2553.

(9) Geng, J.; Jefferson, D. A.; Johnson, B. F. G. *Chem. Commun.* **2004**, 2442.

(10) Pol, S. V.; Pol, V. G.; Frydman, A.; Churilov, G. N.; Gedanken, A. *J. Phys. Chem. B* **2005**, *109*, 9495.

(11) (a) Bandow, S.; Saito, Y. *Jpn. J. Appl. Phys*. **1993**, *32*, L1677. (b) Saito, Y.; Matsumoto, T.; Nishikubo, K. *J. Cryst. Growth* **1997**, *172*, 163.

(12) Teunissen, W.; de Groot, F. M. F.; Geus, J.; Stephan, O.; Tence, M.; Colliex, C. *J. Catal.* **2001**, *204*, 169.

(13) Kim, D. K.; Zhang, Y.; Kehr, J.; Klason, T.; Bjelke, B.; Muhammed, M. *J. Magn. Mater.* **2001**, *225*, 256.

(14) Bystrzejewski, M.; Huczko, A.; Lange, H. *Sens. Actuators, B* **2005**, *109*, 81.

(15) Dyal, A.; Loos, K.; Noto, M.; Chang, S. W.; Spagnoli, C.; Shafi, K. V. P. M.; Ulman, A.; Cowman, M.; Gross, R. A. *J. Am. Chem. Soc.* **2003**, *125*, 1684.

(16) Xu, C.; Xu, K.; Gu, H.; Zhong, X.; Guo, Z.; Zheng, R.; Zhang, X.; Xu, B. *J. Am. Chem. Soc.* **2004**, *126*, 3392.

(17) Xu, C.; Xu, K.; Gu, H.; Zheng, R.; Liu, H.; Zhang, X.; Guo, Z.; Xu, B. *J. Am. Chem. Soc.* **2004**, *126*, 9938.

(18) Ho, K. C.; Tsai, P. J.; Lin, Y. S.; Chen, Y. C. *Anal. Chem.* **2004**, *76*, 7162.

(19) Yang, H. H.; Zhang, S. Q.; Chen, X. L.; Zhuang, Z. X.; Xu, J. G.; Wang, X. R. *Anal. Chem.* **2004**, *76*, 1316.

(20) Hwang, G. L. U.S. Patent 0126303 A1, 2004.

(21) (a) Xie, C. S.; Hu, J. H.; Tao, Z. Y.; Huang, W. Chinese Patent 1240687, 2000. (b) Xie, C. S.; Hu, J. H. Chinese Patent 1250701, 2000.

(22) (a) Niyogi, S.; Hamon, M. A.; Hu, H.; Zhao, B.; Bhowmik, P.; Sen, R.; Itkis, M. E.; Haddon, R. C. *Acc. Chem. Res*. **2002**, *35*, 1105. (b) Balasubramanian, K.; Burghard, M. *Small* **2005**, *1*, 180.

(23) Chen, J.; Hamon, M. A.; Hu, H.; Chen, Y.; Rao, A. M.; Eklund, P. C.; Haddon, R. C. *Science* **1998**, *282*, 95.

(24) Liu, J.; Rinzler, A. G.; Dai, H. J.; Hafner, J. H.; Bradley, R. K.; Boul, P. J.; Lu, A.; Iverson, T.; Shelimov, K.; Huffman, C. B.; Rodriguez-Macias, F.; Shon, Y. S.; Lee, T. R.; Colbert, D. T.; Smalley, R. E. *Science* **1998**, *280*, 1253.

(25) Hamon, M. A.; Chen, J.; Hu, H.; Chen, Y.; Itkis, M. E. Rao, A. M.; Eklund, P. C.; Haddon, R. C. *Adv. Mater*. **1999**, *11*, 834.

(26) Xing, Y. C.; Li, L.; Chusuei, C. C.; Hull, R. V. *Langmuir* **2005**, *21*, 4185.

(27) Ma, Y. W.; Hu, Z.; Huo, K. F.; Lu, Y. N.; Hu, Y. M.; Liu, Y.; Hu, J. H.; Chen, Y. *Carbon* **2005**, *43*, 1667.

(28) Zhang, J.; Zou, H. L.; Qing, Q.; Yang, Y. L.; Li, Q. W.; Liu, Z. F.; Guo, X. Y.; Du, Z. L. *J. Phys. Chem. B* **2003**, *107*, 3712.

(29) Ago, H.; Kugler, T.; Cacialli, F.; Salaneck, W. R.; Shaffer, M. S. P.; Windle, A. H.; Friend, R. H. *J. Phys. Chem. B* **1999**, *103*, 8116.

(30) (a) Okpalugo, T. I. T.; Papakonstantinou, P.; Murphy, H.; McLaughlin, J.; Brown, N. M. D. *Carbon*, **2005**, *43*, 153. (b) Martínez, M. T.; Callejas, M. A.; Benito, A. M.; Cochet, M.; Seeger, T.; Ansón, A.; Schreiber, J.; Gordon, C.; Marhic, C.; Chauvet, O.; Fierro, J. L. G.; Maser, W. K. *Carbon* **2003**, *41*, 2247. (c) Simmons, J. M.; Nichols, B. M.; Baker, S. E.; Marcus, M. S.; Castellini, O. M.; Lee, C. S.; Hamers, R. J.; Eriksson, M. A. *J. Phys. Chem. B* **2006**, *110*, 7113. (d) Kyotani, T.; Nakazaki, S.; Xu, W. H.; Tomita, A. *Carbon* **2001**, *39*, 782.

(31) (a) Moreno-Castilla, C.; Ferro-García, M. A.; Joly, J. P.; Bautista-Toledo, I.; Carrasco-Marín, F.; Rivera-Utrilla, J. *Langmuir* **1995**, *11*, 4386. (b) Ros, T. G.; van Dillen, A. J.; Geus, J. W.; Koningsberger, D. C. *Chem. Eur. J.* **2002**, *8*, 1151.

(32) Chattopadhyay, D.; Galeska, I.; Papadimitrakopoulos, F. *J. Am. Chem. Soc.* **2003**, *125*, 3370.

(33) Basiuk, E. V.; Monroy-Peláez, M.; Puente-Lee, I.; Basiuk, V. A. *Nano Lett.* **2004**, *4*, 863.